Monte Carlo studies of grain boundary segregation and ordering

William L. Alba and K. Birgitta Whaley

Citation: The Journal of Chemical Physics **97**, 3674 (1992); doi: 10.1063/1.462950
View online: http://dx.doi.org/10.1063/1.462950
View Table of Contents: http://scitation.aip.org/content/aip/journal/jcp/97/5?ver=pdfcov
Published by the AIP Publishing

Monte Carlo studies of grain boundary segregation and ordering

William L. Alba and K. Birgitta Whaley
Department of Chemistry, University of California, Berkeley, California 94720

(Received 22 August 1991; accepted 19 May 1992)

This paper describes a systematic microscopic study of solute segregation and ordering at a grain boundary. We develop for this inhomogeneous system several Monte Carlo techniques and apply these to analyze the distribution of substitutional impurities near a symmetric coincident-site-lattice tilt boundary. The calculations demonstrate the importance of ensemble and boundary condition for a Monte Carlo simulation, especially one with an inhomogeneous lattice and with ordering, as opposed to segregating, bulk interactions. The resulting concentration profiles exhibit segregation to the boundary at high temperatures and bulk ordering at low temperature. Based on our results, we propose a mechanism for a solid–solid interfacial ordering phase transition previously suggested by experiment. We also compare these simulations to our earlier one-dimensional mean-field work and find that the three-dimensional simulations confirm the essential mean-field predictions.

I. INTRODUCTION

The segregation of impurities to grain boundaries affects numerous important properties of metals and alloys, such as fracturing, embrittlement, and stress corrosion.[1] While experimental techniques can in principle resolve chemical species on the atomic scale,[2] practical limitations have so far hampered such study. The lateral distribution of segregant species in the boundary region and the effect of this arrangement on metallurgical properties remain unknown.

A recent mean-field model[3] is the first analytic theory to include the effects of both atomic–scale structure and atomic–scale interactions on boundary segregation. As a further step towards developing as microscopic picture of equilibrium grain-boundary segregation, this paper presents an extensive Monte Carlo study of a model Cu(Bi) system. These simulations allow us to investigate the lateral segregant distribution at an atomic level, to understand the role of bulk and boundary structure and atomic interactions, and to discern the relation of phase transitions in the boundary to those in the bulk.

Computer simulations have been used extensively in recent years to study structure, relaxation, and energetics of grain boundaries.[4] For instance, substitutional insertion calculations have made progress in calculating segregation energies, in the limit of infinite dilution of the impurity in the bulk.[5] Monte Carlo simulations of equilibrium segregation have also become increasingly sophisticated, including embedded atom potentials and positional relaxation.[6] However, none of these previous studies involved systems where the bulk forms an ordered structure at low temperature. The simulation of a system which is both spatially inhomogeneous and ordering in the bulk presents novel problems in the choice of Monte Carlo algorithm and boundary conditions. Our efforts to solve this system have been rewarded, however, since we are able to offer an explanation here for the experimental observation of a boundary phase transition in Cu(Bi).[7]

Section II introduces the various Monte Carlo methods. Besides the traditional canonical and grand-canonical Metropolis algorithms, we describe a simulation with a concentration-dependent chemical potential, one with a spatially dependent chemical potential, an umbrella sampling method, boundary condition-driven "pseudocanonical" simulations, and a new kinetic algorithm with several advantages over previous kinetic Monte Carlo methods. We also describe the parameters of our model system here. Section III presents the results of the simulations to characterize bulk Cu(Bi), while Sec. IV, describes results in the presence of a grain boundary, Section V, discusses and summarizes these results in the context of other theories and experiments. In particular, we compare these three-dimensional Monte Carlo simulations to our earlier one-dimensional mean-field results[3] and to a recent experiment[7] which suggests the presence of a boundary phase transition in Cu(Bi).

II. OVERVIEW OF MONTE CARLO METHODS

In this section we review the Monte Carlo methods which we apply to analyze the copper/bismuth system. In the grand-canonical simulations, the bismuth concentration varies, subject to a change in energy due to a chemical potential difference $\delta\mu$. In addition to a concentration-independent $\delta\mu$, we describe methods where $\delta\mu$ depends on concentration and on spatial location. Each of these simulations complements the canonical simulations and helps explain their behavior. We also discuss the use of umbrella sampling[8] and boundary conditions to help control the concentration, as well as a kinetic method which introduces more realistic dynamics.

Most of our simulations employ the Metropolis algorithm to calculate the likelihood of entering a possible state. That is, the energy of a possible state is compared to the energy of the current state; if the former is lower, the move is immediately accepted; if higher, the move is accepted with probability $\exp(-\beta\Delta E)$. (We shall consistently use the notation $\Delta X = X_f - X_i$ for variable X with X_f the final and X_i the initial value.) In the canonical ensem-

 0021-9606/92/173674-14$006.00

ble, a move consists of attempting to exchange the atoms on two neighboring sites chosen at random. Sites in this study are considered to be sufficiently close for exchange if their separation is <3.085 Å, the arithmetic average of the nearest and next-nearest neighbors in a bulk copper crystal. The canonical ensemble is appropriate for finding the most stable configuration of a system at a fixed total concentration.

In the grand-canonical ensemble, a move consists of attempting to change the type of atom on a randomly selected site from copper to bismuth, or vice versa. Because the concentration changes, the energy difference ΔE now also includes a chemical potential difference term $\delta\mu=\mu_{\mathrm{Cu}}-\mu_{\mathrm{Bi}}=(dG/dn_{\mathrm{Cu}}-dG/dn_{\mathrm{Bi}})$. For the traditional grand-canonical simulations, $\delta\mu$ varies with temperature but remains constant over fluctuations in concentration. The energy term therefore depends linearly on impurity concentration.

Both types of simulations present advantages. The grand-canonical simulations can simulate a finite system in contact with an infinite bath of particles. This is particularly important in a spatially inhomogeneous system, such as one with a grain boundary, since the presence of an interface can deplete the local bulk concentration. The grand canonical ensemble in principle can prevent this effect by supplying a uniform environment for the bulk region. Previous simulations[9] attempted to specify the bulk concentration via a different method, by constructing spatial boundary conditions. We have also experimented with controlling the concentration with various boundary conditions and conclude that such methods depend greatly on the boundary size and on the nature of the boundary condition, often lack theoretical or physical justification, and lead to inconsistent results. The canonical simulations, on the other hand, have the advantage of complete control over the system's total concentration without recourse to additional empirical parameters. This straightforward approach is highly desirable when a system forms an ordered bulk phase but must remain at a fixed concentration.

A. Grand-canonical variations

In one variation on the usual grand-canonical method, we include an additional energy term $\chi(c-c_0)^2$ which is quadratic in concentration. This extra term drives the simulation towards a desired concentration c_0. The total energy change in such a simulation is therefore

$$\Delta E=\Delta E_\phi+\delta\mu\Delta c+\frac{\chi}{\beta}\Delta(c-c_0)^2. \tag{1}$$

The first term represents the change in energy due to pairwise interactions and occurs in the canonical as well as grand-canonical simulations. The second term represents the change in energy due to a concentration-independent chemical potential and occurs in any simulation where the concentration varies, while the third term represents the concentration-dependent quadratic potential centered about c_0.

Although simulations typically treat chemical potentials as constant at a given temperature, the chemical potential is more generally a function of concentration. Therefore, one can view this extra term as a chemical potential difference $\delta\mu'(c)$ which depends on concentration, so that the change in energy is

$$\Delta E=\Delta E_\phi+\delta\mu'\Delta c. \tag{2}$$

The form of this new chemical potential difference is

$$\delta\mu'=\delta\mu+2\frac{\chi}{\beta}(\bar{c}-c_0), \tag{3}$$

where $\bar{c}$ is the average between the initial and final concentrations. The special treatment of c_0 by this potential is physically unrealistic, but does allow the simulation to sample configurations which would otherwise occur infrequently.

The implementation of the algorithm is as follows. If a proposed move brings the concentration closer to the desired concentration c_0, that move is accepted with Metropolis probability. Otherwise if a proposed move takes the concentration farther from c_0, the move is accepted with Metropolis probability multiplied by an additional factor $\exp[-\chi\Delta(c-c_0)^2]$. Note that if χ is zero, this simulation is identical to the grand-canonical method above.

We will describe empirical methods to obtain values for $\delta\mu$ and χ in Sec. III A and III B when we detail the results of the simulations. The search for the appropriate $\delta\mu$ corresponding to a desired concentration in the usual grand canonical ensemble will include a simulation where the chemical potential difference varies spatially. Although this situation cannot occur at true equilibrium, such a simulation helps us find $\delta\mu$, provides insight to the problems in simulating an ordering system, and also helps to characterize a phase transition when the concentration varies spatially.

In addition to these variations on the grand-canonical method where the chemical potential difference $\delta\mu$ varies with concentration and over space, we also performed simulations with umbrella sampling and with nonperiodic boundary conditions. Both of these methods attempt to control the concentration further while allowing the simulation to remain in the less constrained grand-canonical ensemble. For the umbrella sampling method, the thermodynamic mean of each property X is calculated according to

$$\langle X\rangle=\frac{\langle X\exp(-\beta U)\rangle_0}{\langle\exp(-\beta U)\rangle_0}, \tag{4}$$

where U is an umbrella potential that preferentially weights configurations closer to the desired concentration c_0. One such scheme is to choose U equal to the third term of Eq. (1). The Boltzmann average $\langle\cdots\rangle_0$ is performed over the grand-canonical ensemble, that is, the first two terms in Eq. (1).

For simulations where boundary conditions are used to influence the concentration, the part of the simulation which is distant from the solid–solid interface is manipulated in a non-Boltzmann fashion to encourage the desired concentration. This type of method has been used previously in the canonical ensemble to control the concentra-

tion of a grain-boundary simulation.[9] We have used similar boundary-condition methods in the canonical and grand-canonical ensembles. Because the nature of the boundary conditions removes the simulation from a proper ensemble, we will refer to these as "pseudocanonical" methods. The results for some of these simulations will be discussed briefly in Sec. IV B when we review the grain-boundary results.

B. Vacancy-oriented kinetic algorithm

In well-defined classical Monte Carlo simulations, the principle of detailed balance assures equilibrium. Namely, suppose that P_i is the probability of the system being in state i and $W_{j\leftarrow i}$ is the conditional transitional probability that the system will move to state j if it is now in state i. Then equilibrium is established when

$$\sum_j (P_i W_{j\leftarrow i} - P_j W_{i\leftarrow j}) = 0 \tag{5}$$

for every state i. As a sufficient (but not necessary) condition for equilibrium, detailed balance assumes the terms in parentheses are satisfied for every pair of states i and j,

$$P_i W_{j\leftarrow i} - P_j W_{i\leftarrow j} = 0. \tag{6}$$

In conjunction with the Boltzmann equilibrium condition, we see that equilibrium will be reached if the transitional probabilities satisfy

$$\frac{W_{j\leftarrow i}}{W_{i\leftarrow j}} = \frac{P_j}{P_i} = \frac{\exp(-\beta E_j)}{\exp(-\beta E_i)} \tag{7}$$

for all i and j. This demonstrates why the Metropolis algorithm achieves equilibrium, and also illustrates that any method which satisfies Eq. (7) is in principle equally valid.

Kinetic Monte Carlo schemes attempt to introduce a stronger dynamic interpretation than traditional Monte Carlo simulations. Instead of choosing a site or pair of sites at random, kinetic algorithms assume that a move has a greater tendency to occur if it is energetically favorable. That is, the rates of the moves are themselves Boltzmann weighted, a situation assumed to more closely resemble physical reality than the random selection of particles made in traditional Monte Carlo. In addition, a kinetic simulation keeps track of time not artificially by the number of attempted moves, but directly, by summing the rates to produce a total rate and randomly selecting a time under the assumption that the total rate is described by a Poisson distribution. Binder[10] more fully describes the theory and practice of kinetic Monte Carlo.

In our kinetic algorithm, we begin by replacing the bismuth or copper atom at a random site with a vacancy, a common type of point defect. In physical systems, the movement of such holes through a crystal lattice is often the predominant mechanism for atomic mobility.[11] Assuming without loss of generality zero interaction energy between a vacancy and a bismuth or a copper atom, we calculate the energy before and after exchanging the vacancy with neighboring atom. Then the rate of exchange of the vacancy with a neighboring site i is

$$r_i = \min[\exp(-\beta \Delta E), 1], \tag{8}$$

where ΔE is the difference between the final and initial energies of the proposed exchange. The rate expression is analogous to the acceptance criterion in the Metropolis algorithm and, surprisingly, serves for our system better than an alternative rate based only on the final energy after exchange $r_i = \exp(-\beta E_f)$. This second expression, which also satisfies detailed balance, is larger for energies which are lower than the initial energy, so it was expected to reach equilibrium more quickly. Both of these definitions for the rate satisfies the condition of detailed balance, since they are essentially the conditional probabilities $W_{j\leftarrow i}$ of Eq. (7).

The total rate of exchange for the vacancy is the sum of the individual rates

$$R = \sum_i r_i, \tag{9}$$

where the sum is restricted over neighboring sites. We then select which exchange to perform by taking the lowest i' which satisfies

$$\frac{\sum_{i=1}^{i'} r_i}{R} \geq \Gamma, \tag{10}$$

where Γ is a random number uniformly distributed between 0 and 1. Assuming the next vacancy exchange occurs with a Poisson distribution, the time elapsed between successive moves is

$$t = -1/R \log(\Gamma). \tag{11}$$

To avoid possible artificial correlations, a second random number is used for the elapsed time.

This vacancy-oriented algorithm is not only physically motivated, but it also possesses several advantages over other Monte Carlo schemes. Previous kinetic Monte Carlo algorithms[10] required calculating and keeping track of a much larger number of rates. When two particles are moved in such algorithms, the exchange rate for every site within the interaction range of the pair with all of its own exchange neighbors would have to be recalculated. In our algorithm, because only the vacancy moves, we need calculate the exchange rates of only the vacancy with its neighbors. If the number of exchange neighbors is n_{exch} and the number of interaction neighbors is n_{int}, then other kinetic algorithms require on the order of $n_{\text{int}}^2 n_{\text{exch}}$ pairwise energy evaluations, while the vacancy-oriented algorithm requires on the order of $n_{\text{int}} n_{\text{exch}}$ evaluations. For our face-centered cubic system, we allow nearest-neighbor exchanges in the bulk and cut off the potential at the fourth-nearest neighbor, so $n_{\text{int}} = 54$ and $n_{\text{exch}} = 12$. Since we have assumed that the vacancy-particle energy is zero, we need to calculate only half the usual pairwise interactions. Thus, compared to other kinetic methods, our algorithm decreases the time per step by two orders of magnitude.

Although the number of energy calculations here is still $n_{\text{exch}}/2$ times greater than traditional Metropolis Monte Carlo, this vacancy-oriented algorithm can be interpreted to allow examination of the kinetics of a bound-

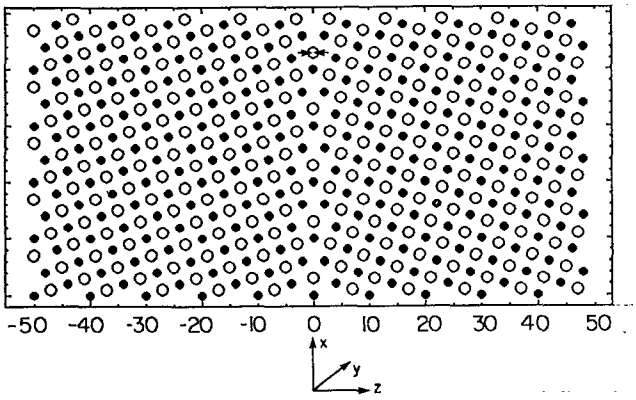

FIG. 1. A sample bicrystal computational cell. Each circle represents a site for bismuth or copper. Two planes are shown, the small dark circles lie 1.807 Å below the large circles. These two atomic planes repeat along the x-direction. At the central grain boundary plane, two sites which would have been 1.14 Å apart are eliminated and replaced by one site at the central layer, as indicated by the arrows.

ary phase transition. Also, although each Monte Carlo move is less efficient computationally, at low temperature this scheme should prove more effective than the Metropolis algorithm, since a move is always performed (the vacancy always migrates). We thereby avoid the critical slowing-down[10] which occurs in other canonical simulations as the acceptance rate decreases.

C. Copper/bismuth geometry and interactions

The geometry and interactions of our model copper/bismuth system are fully described in a previous paper,[3] so we discuss these here only briefly. Copper/bismuth is a binary system with simple empirical potentials available,[12] a high degree of experimentally observed bismuth segregation[13] and experimental indication of a boundary phase transition.[7] The segregation of substitutional bismuth impurities to copper grain boundaries causes embrittlement in copper.[14]

Since our system is a high-angle symmetrical tilt boundary, its structure is well-represented by the coincidence site lattice (CSL) model.[15] In the CSL model, on both sides of the boundary is a face-centered cubic crystal with the lattice parameters of bulk copper (nearest-neighbor distance 2.556 Å). A small number of atoms coincident with the lattice positions of both crystals forms the center of the boundary (Fig. 1). We make one modification to the CSL, which is to treat the two atomic sites adjacent to the interface, which would have been 1.14 Å apart and resulted in unrealistically excessive repulsive interactions, as a single site at an intermediate distance at the center of the grain boundary. The tilt angle is $\sim 36.87°$ around the $\langle 100\rangle$ axis, yielding a reciprocal volumetric density of coincidence sites of $\Sigma=5$. The grain boundary and the atomic layers parallel to it are $\langle 210\rangle$ planes. At this time, we do not permit lattice relaxation and this will allow us to make a direct comparison with our earlier mean-field results.[3]

The simulations use periodic boundary conditions along all three spatial dimensions. A typical bulk simulation contains 240 layers along the z-dimension (see Fig. 1), corresponding to 137.1 Å in that direction. The x and y-dimensions typically measure 28.6 and 10.8 Å, and a bulk crystal of these dimensions contains 3600 sites. In the grain-boundary simulations, imposing periodic boundary conditions results in two identical tilt boundaries along the planes where the crystals adjoin. In order to maximize the separation between these boundaries and to gather the most information as a function of distance from a boundary, the largest dimension of the simulation is again taken in the z-direction perpendicular to the boundary. A typical grain-boundary simulation contains 260 layers, measures 148.6 Å by 28.6 Å by 10.8 Å, and holds 3870 sites.

Each lattice site contains a copper (bulk) atom or a bismuth (impurity) atom. The atoms interact pairwise via Morse potentials truncated at the fourth-nearest-neighbor bulk distance

$$\phi(r)=D\{\exp[-2\alpha(r-\beta)]-2\exp[-\alpha(r-\beta)]\}. \tag{12}$$

Parameters of the Morse potentials for copper–copper, bismuth–bismuth, and copper–bismuth are given in Ref. 3, where the potentials are also plotted showing the bulk and grain boundary-induced interactions.

The Hamiltonian for our binary alloy is

$$\mathcal{H}=1/2\sum_i\sum_j[\phi_{ij}^{\mathrm{Bi-Bi}}(r)c_i^{\mathrm{Bi}}c_j^{\mathrm{Bi}}+2\phi_{ij}^{\mathrm{Bi-Cu}}(r)c_i^{\mathrm{Bi}}c_j^{\mathrm{Cu}} +\phi_{ij}^{\mathrm{Cu-Cu}}(r)c_i^{\mathrm{Cu}}c_j^{\mathrm{Cu}}]+\sum_i(c_i^{\mathrm{Bi}}\mu^{\mathrm{Bi}}+c_i^{\mathrm{Cu}}\mu^{\mathrm{Cu}}). \tag{13}$$

Here $\phi_{ij}^{X-Y}(r)$ corresponds to the Morse potential between species X at site i and species Y at site j, which depends only on $r=|\mathbf{r}_i-\mathbf{r}_j|$ (ϕ_{ii}^{X-Y} is defined to be zero); μ^X corresponds to the chemical potential of species X and is assumed uniform over the bicrystal lattice at equilibrium; and c_i^X corresponds to the occupation number of species X at site i. The latter is either zero or unity at each site, so that c^{Bi} is 1 and c^{Cu} is 0 when bismuth occupies site i, and $c^{\mathrm{Bi}}=1-c^{\mathrm{Cu}}$.

For convenience, we define a normalized temperature $T^*=2kT/(D^{\mathrm{Cu-Cu}}+D^{\mathrm{Bi-Bi}}-2D^{\mathrm{Bi-Cu}})$, where the D's are the Morse potential depth parameters. Each degree of normalized temperature equals 2646 K. All simulations start at $T^*=12$ with a random configuration of copper and bismuth atoms, subject to the requirement that each layer perpendicular to the grain boundary has a bismuth concentration near 15%. The temperature is then lowered successively by a constant multiplicative factor (0.84), with 8×10^6 Monte Carlo moves at each temperature. After 15 different temperatures, when the simulation is at $T^*=1.05$, the ratio of successful Monte Carlo moves to unsuccessful ones becomes prohibitively small, and we halt the simulation.

Although the simulation occurs above the melting points of copper and bismuth, the equilibrium structure at

the experimental solid temperatures is likely to be the structure which we observe at the lowest temperatures in our simulations. The Metropolis algorithm slows down considerably at lower temperatures because as we approach experimental freezing temperatures, atomic mobilities then typically decrease by orders of magnitude. In order to achieve equilibrium profile statistics with Monte Carlo techniques within a reasonable time, we must work at a high enough kT so that atomic mobility is still relatively fast. For similar reasons, our simulations are run with bismuth concentrations of 5% to 25%, even though the equilibrium concentration of bismuth in copper is 1%.[16] Since the local concentration in the vicinity of a grain boundary may be much higher than the equilibrium bulk concentration[13] and since we are also concerned with the development of general techniques in addition to the specific behavior of the copper/bismuth system, this is not a problem for the present study.

We can also write our binary alloy Hamiltonian as a general Ising model,

$$\mathcal{H}=-1/2\sum_i\sum_j J_{ij}s_is_j-\sum_i H_is_i+C, \tag{14}$$

where J_{ij} is the spin–spin coupling between the spins at sites i and j, H_i is the coupling between the magnetic field and the spin at site i, C is a constant term, and the spin variable s_i on site i takes on values of ± 1. By translating the bismuth concentration variable c_i^{Bi} to the spin variable s_i,

$$c_i^{\mathrm{Bi}}=1/2(1+s_i), \tag{15}$$

we relate the binary-alloy Hamiltonian terms to the corresponding spin-model terms,

$$J_{ij}=1/2[\phi_{ij}^{A-B}-1/2(\phi_{ij}^{A-A}+\phi_{ij}^{B-B})], \tag{16}$$

$$H_i=1/4\sum_j(\phi_{ij}^{B-B}-\phi_{ij}^{A-A})+1/2(\mu^B-\mu^A). \tag{17}$$

We also define a layer–layer coupling,

$$\langle J_{nn'}\rangle=\sum_{j_{n'}}J_{i_nj_{n'}}. \tag{18}$$

The summation is restricted, requiring that site i is in the nth layer and each site j is in the n'th layer.

The translational symmetry breaking introduced by the grain boundary causes J_{ij}, H_i, and $\langle J_{nn'}\rangle$ to depend in an atypical fashion on the z coordinate, namely, on the distance from the grain boundary. For this particular system, the behavior of H_i indicates that bismuth will be present only in small amounts and will segregate to the grain boundary. Our one-dimensional mean-field analysis shows that the magnetic field H_i largely determines the high-temperature structure of the segregant, while at lower temperatures $\langle J_{nn'}\rangle$ also influences the segregant structure. For a full discussion and derivation of these results, we refer the reader to our earlier paper.[3]

In Sec. III, we apply the Monte Carlo methods described above to a Cu(Bi) bulk system. Among the grand-canonical methods in the bulk, we apply the Metropolis algorithm with a spatially constant and also with a linearly varying chemical potential difference. We also describe the results of the canonical Metropolis algorithm in the bulk. In Sec. IV, we apply the Monte Carlo methods to a Cu(Bi) system with two grain boundaries. In the grain-boundary case, we will discuss the results and address the difficulties of various grand-canonical methods, including the Metropolis algorithm, the use of the concentration–dependent chemical potential difference and of umbrella sampling, and "pseudocanonical" methods which depend on boundary condition. Finally, we apply the two most viable methods, Metropolis canonical and vacancy-oriented kinetic Monte Carlo, to the grain-boundary system.

III. BULK SIMULATIONS: RESULTS AND DISCUSSION

Our general aim is to obtain equilibrium segregation distributions over a range of temperatures and concentrations, both perpendicular and parallel to the grain boundary. However, before considering the behavior at the solid–solid interface, we will broadly characterize the pure bulk phase to provide a reference for the bulk portion of the grain-boundary system. In this section we present Monte Carlo results in the grand-canonical and canonical ensembles and indicate the computational complexity of this ordering system, even in the absence of a grain boundary.

A. Metropolis grand-canonical

In these grand-canonical simulations, the total number of particles is constant, but the concentration of each species varies. Because the Morse potentials of our system favor the absence of bismuth, we apply a spatially uniform chemical potential difference, $\delta\mu=\mu^{\mathrm{Cu}}-\mu^{\mathrm{Bi}}$, to encourage its presence. From Eq. (17), this is equivalent in the isomorphic Ising system to applying an additional uniform external magnetic field to partly offset the external magnetic field due to the Morse potentials.

Application of the correct chemical potential difference over the entire lattice should in principle allow control of the bismuth concentration over the entire range from zero to unity. To achieve good statistics, we would like to apply a chemical potential difference which gives a bismuth concentration of $\sim$10–20%. A grand-canonical simulation without a chemical potential difference to force bismuth into the system finds the correct physical result,[16] that the equilibrium bismuth concentration in the system is 1%, except at very high temperature, when entropic effects favor a random 50/50 mixture.

As a first approximation to find the appropriate chemical potential difference corresponding to a given bismuth bulk concentration, we use the regular solution model. To account for interactions beyond nearest neighbor in the regular solution model, we replace J in the usual formulation by the sum over all distances r of $J_{ij}(r)$, up to the cutoff potential range. This is equivalent to our one-dimensional mean-field theory when the phase is paramagnetic.[3] However, one cannot expect a zero or one-dimensional model to give a precise value for $\delta\mu$, especially for a three-dimensional system with an extended range of frustrated and ordering interactions, and indeed we must

TABLE I. Chemical potential differences $\delta\mu=\mu^{Cu}-\mu^{Bi}$.[a]

T^*	Regular solution	Monte Carlo
12.00	0.88	2.25 (0.121)
5.97	3.26	11.75 (0.120)
2.98	4.45	15.50 (0.122)
1.76	4.93	15.75 (0.209)

[a]Chemical potential differences in eV. For the Monte Carlo simulations, the actual bulk concentration is given in parentheses.

adjust the above derived value for $\delta\mu$. We therefore made short Monte Carlo runs at each temperature to determine the actual chemical potential difference appropriate for the desired bismuth concentration. Table I summarizes for each temperature the values of $\delta\mu$ necessary for a bulk bismuth concentration of $\sim 15\%$ and the actual bismuth concentration in the simulation.

At low temperatures ($T^*\approx 3$ and below), we encounter difficulty in bringing the bismuth concentration to the range 10–20%. Instead, over a small range of $\delta\mu$, we find either a complete absence of bismuth, or one of two ordered phases which each average 25% bismuth. The first type of ordered domain is antiferromagnetic (alternating atomic planes of approximately 0% and 50% bismuth), while the second is a $\lambda=6$ ordered phase (three atomic planes of 16.7% bismuth followed by three atomic planes of 33.3% bismuth).

The sensitivity of concentration to small changes in $\delta\mu$ reflects the appearance of a state in which this 25% bismuth antiferromagnetic phase and a pure copper phase coexist. In an infinite-sized system, the chemical potential could control the bismuth concentration by varying the sizes and relative amounts of the regions containing the 25% bismuth phase and the 0% bismuth phase. However, this finite-sized grand-canonical simulation only shows either of these phases, but not both simultaneously. The appearance at low temperature of the ordered phase and the pure copper phase is even sensitive to the random-number seed and to the size of the simulation.

The appearance of only one phase in a small system when a mixture of two phases is stable in the infinitely sized limit apparently occurs in other computations as well. In some molecular dynamics simulations by Berry and co-workers,[17] single rare-gas clusters can appear alternately as a gaseous phase and a liquid phase. Presumably, in the thermodynamic limit, some regions of space resemble the gaseous phase while others resemble the liquid phase. Similarly, in our ordering system there exists a $\delta\mu$ corresponding to 15% bismuth which in the infinite system would be filled with the appropriate ratios of domains of an ordered phase (25% bismuth) and of the pure copper phase (0% bismuth). But in a finite system at that $\delta\mu$, we settle into either the ordered phase or the pure copper phase and, unlike the rare-gas cluster simulations, the slow dynamics of this solid system prevents us from observing an alternation of these phases in "time."

Figures 2(a) and 2(b) show typical low-temperature concentration profiles of the bulk grand-canonical simulation. These figures and all other concentration profiles show the fraction of sites occupied by bismuth in a series of ⟨210⟩ planes. In the presence of a grain boundary, these planes are perpendicular to the interface, so that the profiles then show the behavior of bismuth as a function of distance z from the boundary. Since the two planes adjacent to the coincident site plane are vacant (Fig. 1 and Sec. II A), for graphical purposes the concentration for each of those two planes is assumed to be an average of its two neighboring layers. As described in Sec. II C, the planes adjacent to the central boundary layer contain no sites, so the concentration in these vacant layers is always zero.

These figures and the other bulk and boundary concentration profiles represent average configurations. During a given temperature the system is sampled once every 100 Monte Carlo steps. The first 5×10^5 steps are discarded, to ensure the system is fully equilibrated when calculating the average. Thus, for a typical run with 8×10^6 steps per temperature, each profile represents an average of 75 000 states.

Figure 2(a) occurs at $T^*=2.50$, near the transition temperature for the $\lambda=6$ and antiferromagnetic ordered phases. Both phases coexist at this temperature. Figure 2(b) occurs at $T^*=1.79$, where the $\lambda=6$ phase has grown at the expense of the antiferromagnetic domain and now dominates over the entire system. The appearance of these two particular ordered phases, the approximate value of the transition temperature, and the stability of the $\lambda=6$ phase vs the metastability of the antiferromagnetic phase all confirm predictions made earlier by our one-dimensional mean-field theory.[3]

B. Metropolis grand-canonical with varying $\delta\mu$

Both the simulation described in Sec. III A and the one-dimensional mean-field theory occurred in the grand-canonical ensemble. Both methods therefore encountered difficulty controlling the bismuth concentration at low temperature due to the appearance of ordered phases. To demonstrate further the difficulties with controlling the concentration of a finite system when the infinite system contains two types of ordered domains, we performed a series of grand-canonical simulations where $\delta\mu$ varies linearly across one spatial dimension. Such a method of varying the chemical potential has been used previously[18] to study a system with a segregating, as opposed to ordering, bulk interactions.

Although chemical potentials should strictly be spatially homogeneous at equilibrium, the results of this simulation illustrate how a small change in $\delta\mu$ can significantly alter the behavior of this Cu(Bi) system. Throughout the simulation, the chemical potential $\delta\mu$ increases linearly by 0.96 eV from layer 0 to layer 50, and, to maintain the periodic boundary condition, decreases back down to layer 100. Figure 2(c) shows a concentration profile at $T^*=2.49$. At this temperature, an ordered antiferromagnetic phase just begins to appear at the center of the simulation in the region of high bismuth concentration. At this and at higher temperatures, the concentration of the paramagnetic phase can be well controlled by the chemical

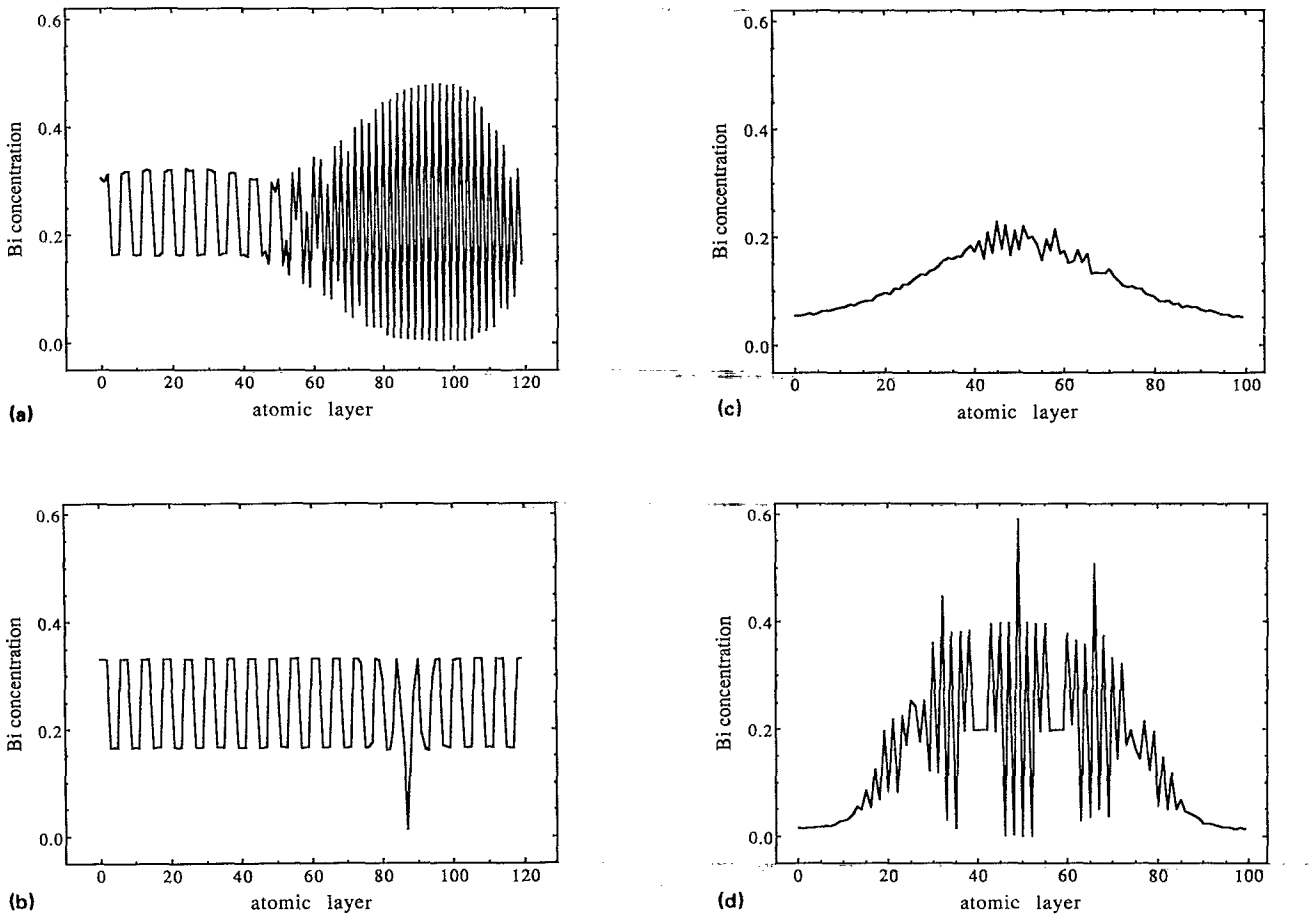

FIG. 2. Concentration profiles of Monte Carlo simulations of bulk copper/bismuth in the grand canonical ensemble. Each graph depicts the concentration of bismuth in ⟨210⟩ planes. (a) and (b) display typical low-temperature ($T^*=2.50$ and 1.79) profiles under the Metropolis algorithm. (c) and (d) display profiles at the same temperatures when the chemical potential difference $\delta\mu$ varies linearly over the lattice.

potential. On the other hand, Fig. 2(d) shows a concentration profile at $T^*=1.79$, well below the transition temperature. We can observe here why the chemical potential can no longer control concentration in this finite system. The central layers of the simulation, subject to high $\delta\mu$, contain an ordered phase, while the farthest layers, which experience low $\delta\mu$, are pure copper. The concentration rises quickly in the region between these two phases, indicating that bismuth concentrations between 0% and 25% are unstable in this finite system. Indeed, under different simulations with increasingly smaller values of $\delta\mu/kT$ over the same number of layers, we have been unable to obtain a structure with a concentration far from either 0% or 25%.

Despite these difficulties with a grand-canonical simulation of an ordering system, for spatially inhomogeneous systems such as those with a grain boundary, it is nevertheless advantageous to be able to control the bulk concentration as if it were in contact with an infinite bath of impurity particles. Therefore, in Secs. IV A and IV B we describe several other ways to maintain the bulk concentration in the presence of depletion by interfacial segregation.

C. Metropolis canonical

The problems of maintaining a particular impurity concentration are absent in the canonical ensemble. Figures 3(a)–3(c) display concentration profiles for the bulk at temperatures above ($T^*=12.00$), near ($T^*=2.98$), and below ($T^*=1.05$) a bulk phase transition temperature. The total concentration of bismuth in these systems is maintained at 15%. As expected from analysis of the grand-canonical results, we observe scattered domains of ordered structures. Besides the antiferromagnetic 50/0% bismuth ordered phase, we also see regions of approximately 25% and 0% bismuth as well as domains where the ordered structure has varying wavelength.

To characterize these structures more precisely and to determine the transition temperature quantitatively, we calculate an order parameter by taking discrete Fourier coefficients of these profiles. For a given wavelength λ (or wave number $q=2\pi/\lambda$), we define

$$a_\lambda = 2/L \sum_{z=0}^{L} S_z \cos(qz), \tag{19}$$

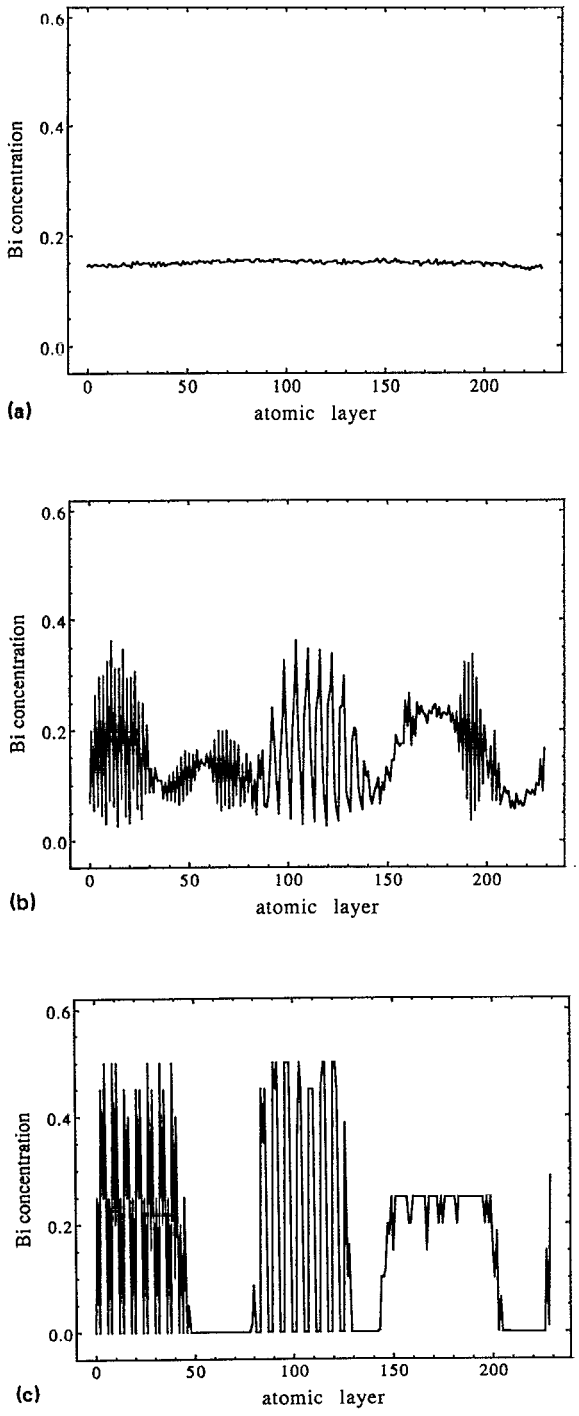

FIG. 3. Concentration profiles of Monte Carlo simulations in the bulk under the canonical ensemble. Each of these was run with the Metropolis algorithm. (a) is at $T^*=12.00$, above the transition temperature; (b) is at $T^*=2.98$, close to the transition temperature; and (c) is at $T^*=1.05$, below the transition temperature.

$$b_\lambda = 2/L \sum_{z=0}^{L} S_z \sin(qz). \tag{20}$$

As before, z is the coordinate perpendicular to ⟨210⟩ planes (Fig. 1), and S_z is the spin variable translation of the bismuth concentration in that plane [Eq. (15)]. In principle, one can reconstruct the profile

$$S_z = \sum_{\lambda=1}^{L} [a_\lambda \cos(qz) + b_\lambda \sin(qz)]. \tag{21}$$

In practice, however, we calculate the Fourier coefficients a_λ and b_λ across the entire lattice, and its length L is not necessarily an integral multiple of a particular wavelength λ. Strictly speaking, these incommensurate λ's should not contribute to the reconstruction of a profile with periodic boundary conditions, but from a physical standpoint we do not wish to arbitrarily exclude the possibility of order with certain periodicity simply because that wavelength is incommensurate with our simulation size. Therefore, we also evaluate Eqs. (19) and (20) for these incommensurate λ's, for which Eq. (21) no longer holds. An order parameter based on those coefficients will then be most accurate for small wavelengths (and will remain correct for all commensurate wavelengths). Since this is a finite system with periodic boundary conditions, we are limited to small wavelengths in any case, so this is a minor restriction.

We can now define an order parameter

$$\Theta_\lambda = a_\lambda^2 + b_\lambda^2, \tag{22}$$

which indicates the amplitude-weighted presence of an ordered structure with wavelength λ. This order parameter operates regardless of phase shifts, so we do not have to concern ourselves with phase boundary domains as one sometimes does with other long-range order parameters.[19,20] For example, suppose the spin profile S_z is sinusoidal with amplitude A, wave number q, and phase factor ζ: $A\sin(qz+\zeta)$. Then from Eqs. (19)–(22), $a_\lambda = A\sin\zeta$ and $b_\lambda = A\cos\zeta$, so $\Theta_\lambda = A$. Since any profile can be written in terms of a Fourier sum of such sine waves, the phase factor in general presents no problem.

Figure 6(a) shows the concentration-profile Fourier coefficient Θ_λ vs temperature for wavelengths $\lambda=2$–9 for the bulk system calculated with the canonical Metropolis method. As expected from examining the concentration profile in Fig. 3(c), we observe a $\lambda=2$ (antiferromagnetic) phase of layers alternatingly rich and deficient in bismuth. The $\lambda=6$ phase also develops strongly, which is not so readily apparent from the profiles. This and other canonical bulk runs indicate that these two ordered phases first appear at a temperature between $T^*=3.54$ and 2.98.

Mean-field theory had previously predicted the appearance of these bulk ordered phases.[3] According to that analysis, the $\lambda=7$ phase is most stable from approximately $T^*=3.54$ to 2.50, $\lambda=6$ is most stable from approximately $T^*=2.10$ down to zero temperature, and the $\lambda=2$ antiferromagnetic phase remains in that temperature range metastable but close in energy to the most stable phase. Given that the mean-field theory is one-dimensional, these temperatures and ordered structures correspond remarkably closely to those of the three-dimensional simulations here.

A zero-temperature three-dimensional calculation of the relative energies of various pure square-wave phases (alternatingly 100/0% or 50/0% bismuth) also reveals that $\lambda=2$ and 6 have by far the lowest energy for all wavelengths up to $\lambda=16$. Without our Morse interactions, these two phases are nearly identical in energy at zero tempera-

ture. For variously sized lattices up to $L=240$, $\lambda=6$ is most stable when L is commensurate with 6, while $\lambda=2$ is otherwise more stable, substantiating the mean-field prediction that for this system these two ordered phases are close in energy.

For each of these simulations, we verify that the energy is well-behaved and that the temperature-normalized energy decreases with temperature. Fluctuations in the energy correspond to the heat capacity

$$C_v=\frac{1}{kT^2}\sqrt{\langle(E-\langle E\rangle)^2\rangle} \tag{23}$$

which serves as an additional order parameter to help locate the phase transition temperature. The heat capacity, shown in Fig. 6(c), peaks sharply near $T^*=3$, indicating the phase transition occurs near that temperature. It therefore confirms the transition temperature range given by the Θ_λ analysis.

Both these order parameters indicate a transition temperature in the canonical ensemble which is approximately the same as that observed in the grand-canonical ensemble ($T^*\approx 3$). In addition to the effect of concentration on the transition temperature, we have also, in the $\delta\mu$ gradient simulations, observed the effect of a concentration gradient.

In summary, as predicted earlier by our one-dimensional mean-field theory, the $\lambda=2$ and 6 phases are the most stable bulk phases. These phases appear most distinctly in the concentration profiles under the grand-canonical ensemble. Furthermore, the heat capacity and concentration-profile Fourier transforms confirm that these phases appear in both the canonical and grand-canonical simulations when $T^*\approx 3$.

IV. BOUNDARY SIMULATIONS: RESULTS AND DISCUSSION

Having determined the main characteristics of the ordering phase transition in the bulk, we now examine the system in the presence of a grain boundary. Because impurities segregate to the interface and yet we wish to maintain the environment of an infinitely sized bulk system, we first describe two grand-canonical simulations, with a concentration-independent and with a concentration-dependent chemical potential difference $\delta\mu$. We briefly describe two alternate methods to control the concentration of the simulation, via umbrella sampling and via modification of the boundary conditions. We then present two simulations in the canonical ensemble, namely, a traditional Metropolis algorithm and our vacancy-oriented kinetic algorithm.

A. Metropolis grand-canonical

Figures 4(a) and 4(b) show typical high and low-temperature concentration profiles for a Metropolis grand-canonical simulation of a grain-boundary system. Figure 4(a), at $T^*=12.00$, clearly shows the general phenomenon of bismuth segregation to the interface. The total amount of segregant increases with lower temperature, together with the width and height of the segregant peak. The segregant peak in this copper/bismuth system also shows fine structure, as suggested previously by experiment,[7] simulation,[9] and analytic theory.[3] The mean-field theory explains the appearance of the characteristics of the segregant peak by examining the magnetic field [Eq. (17)] for this system

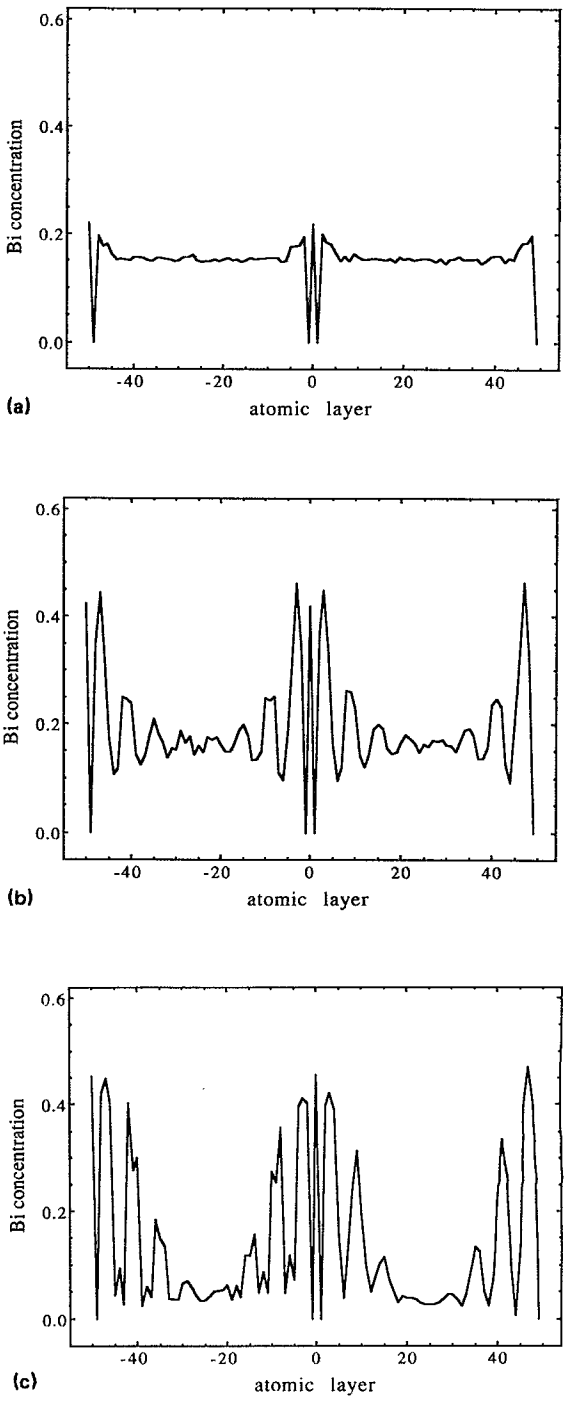

FIG. 4. Concentration profiles of the grain-boundary system in the grand-canonical ensemble. (a) and (b) were run with the traditional Metropolis algorithm, while (c) used a concentration-dependent $\delta\mu$. (a) represents a high-temperature configuration ($T^*=12.00$), while (b) represents a low-temperature configuration ($T^*=2.98$). (c) displays the ability of the additional χ energy term to maintain the concentration near 15% at lower ($T^*=1.79$) temperature.

and showing that the high-temperature structure of a segregant peak is largely determined by the z-dependence of the field.

At lower temperatures (e.g., at $T^*=2.98$) the concentration becomes difficult to control with a concentration-independent $\delta\mu$, as was observed in the pure bulk system (Sec. III A). At $T^*=12.00$, the average concentration per layer is 15.24%, but at this lower temperature, the value has become 19.31%. Furthermore, the bulk ordered phase appears to dominate the entire system, overwhelming any segregant structure at the interface [Fig. 4(b)]. The mean-field analysis showed that the layer–layer coupling dominates over the external field-layer coupling, so that details due to grain boundary structure wash out and the bulk phase appears across the entire simulation.[3] The mean-field theory, which was also made in the grand-canonical ensemble, also predicts the domination of the bulk phase across an interface.

B. Grand-canonical variations

In this section we describe three more variations on the usual grand-canonical simulation, besides the spatially varying chemical potential difference. Each of these is designed to bring the simulation to a more tightly controlled concentration yet allow the freedom of the grand-canonical ensemble which simulates contact with an infinite bulk.

One way to exert greater control over the bulk concentration is to apply an additional concentration-dependent energy term. As described in Sec. II A, this may be viewed as a chemical potential difference $\delta\mu$ which now depends on concentration. Even with the additional χ term [Eq. (1)], at low temperature the concentration in this simulation continues to be attracted to either 0% or 25%. This behavior further confirms that ordered phases at these two concentrations are stable, so that in an infinite system concentrations between 0% and 25% bismuth are represented by the appropriate proportions of those two phases. A large value of χ was necessary to keep the bismuth concentrations near 15%. For the simulations shown in Figs. 4(c) and 4(d), $\chi\approx 90\,500$. This value is so large that, independent of energy considerations, the probability $\exp[-\chi\Delta(c-c_0)^2]$ of increasing the concentration from 15.23% by changing one site from copper to bismuth is only 1%.

Two types of simulations were produced with the concentration-dependent potential. In the first, we apply the potential equally over the entire system; in the second, we separate the lattice into two types of regions, a "boundary" region where the concentration depends only on the Morse potentials and chemical potential difference, and a "bulk" region where the concentration is also subject to the additional potential. The simulation depicted in Fig. 4(c) is of the first type.

As seen in Fig. 4(c), the additional χ term does help to bring the concentration closer to 15% at temperatures lower than the traditional grand-canonical simulation. As with that previous simulation [Figs. 4(a) and 4(b)], we observe segregation to the grain boundary and ordering of the segregant near the interface. However, below $T^*=1.79$, even with this high value for χ, the profiles begin to display an ordered phase with high (25%) concentration in one bulk section of the simulation, and low (0%) concentration in the other bulk section. Making the chemical potential difference strongly depend on the concentration only delayed the effect of this phase transition. The additional energy term has simply forced the ordered phase and the 0% bismuth phase to coexist, a result already seen in the bulk canonical simulation [Fig. 3(c)].

In order to force this simulation to supply consistent concentration to each side of the grain boundaries, we have, as mentioned earlier, also adjusted the boundary conditions. Instead of applying the χ potential over the entire lattice, we apply the additional term separately to two bulk regions. The manipulation of the boundary conditions for these purposes results in what we call "pseudocanonical" simulations. However, this type of simulation relies on an artificial distinction between "bulk" and "grain boundary" regions, and mismatches in concentration occurred between the layers at the interface between those two regions. The undesirable concentration fluctuations between regions was much less pronounced than in the simulations of Chang *et al.*[9] However, all the simulations described in Secs. IV C and IV D below are far better since they avoid such artificial distinctions.

Because of its quadratic dependence about c_0, the additional energetic term in Eq. (1) can also be conveniently used across the entire lattice as an umbrella sampling potential. In this third method to control the concentration, the configurations are weighted so that those with concentrations close to c_0 are accorded greater importance, with a normalization factor to account for the new weighting scheme. Unfortunately, at high temperatures this additional potential makes little difference, since we already have fine control over the concentration, while at low temperature the system "freezes" into configurations whose concentrations are too far from c_0 for the umbrella potential to get a proper sample. The behavior of this simulation differs significantly from that of the traditional grand-canonical simulation only at one temperature $T^*=2.98$, i.e., near the transition temperature. At that temperature, umbrella sampling does dampen the large fluctuations in concentration.

Each of these simulations further illustrates the acute difficulties to control concentration in a finite system with an ordering potential. Together they demonstrate the necessity of using only the canonical ensemble when control over the concentration is required for this system.

C. Metropolis canonical

The bulk simulations in the canonical ensemble at different concentrations, the bulk simulations in the grand-canonical ensemble (especially the linearly varying $\delta\mu$ studies), and the various methods to control more strictly the concentration have shown that only the canonical ensemble can satisfactorily control the concentration of this system with its ordering potentials. However, the use of the canonical ensemble for a problem with both spatially varying potentials and geometry is unfortunate, since the be-

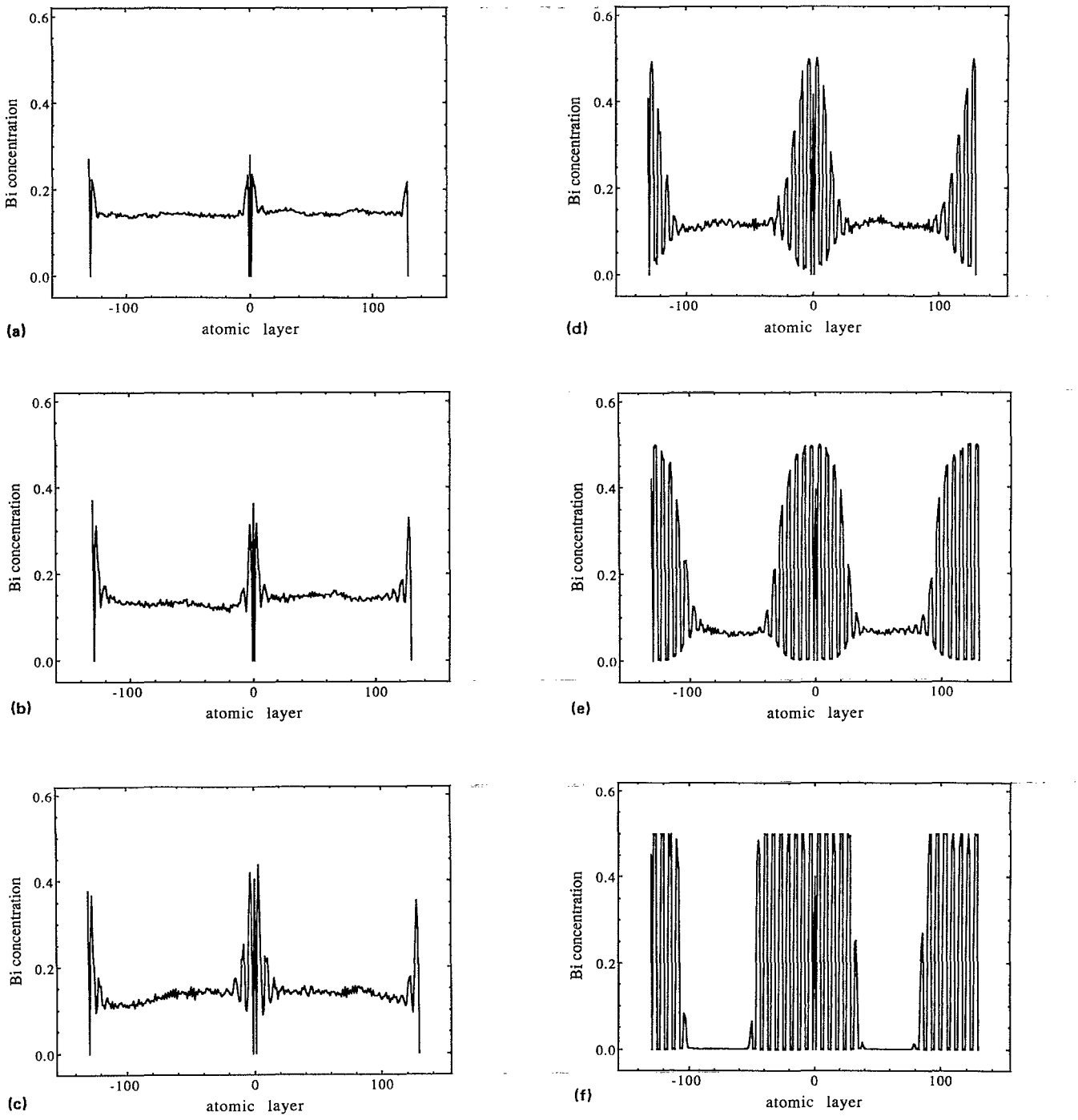

FIG. 5. Concentration profiles of the grain-boundary system in the canonical ensemble with the Metropolis algorithm. (a)–(f) Correspond, respectively, to $T^*=5.97$, 3.54, 2.98, 2.50, 2.10, and 1.05.

havior of the system will then depend somewhat on the size of the simulation. In particular, for our grain-boundary system, the amount of segregant at the interface depends on the amount of bismuth available and, according to empirical segregation theories,[21] to the amount of bismuth remaining in the bulk. Since both these variables depend on the number of sites, a simulation in the canonical ensemble will also depend on grain size. The dependence of segregant behavior on grain size would itself make an interesting study, but for now we choose a grain large enough so that a small increase in size does not cause a large difference in the behavior of the concentration profile, even though the bulk may become depleted in bismuth. A system with 74.3 Å (130 layers) between grain boundaries is sufficiently large for these purposes.

Several runs were performed, and Figs. 5(a)–5(f) depict the concentration profiles from the run with the lowest energy, over a span of temperatures ($T^*=5.97$, 3.54, 2.98, 2.50, 2.10, and 1.05) for the canonical grain-boundary system. In Fig. 5(a) we see the familiar high-temperature

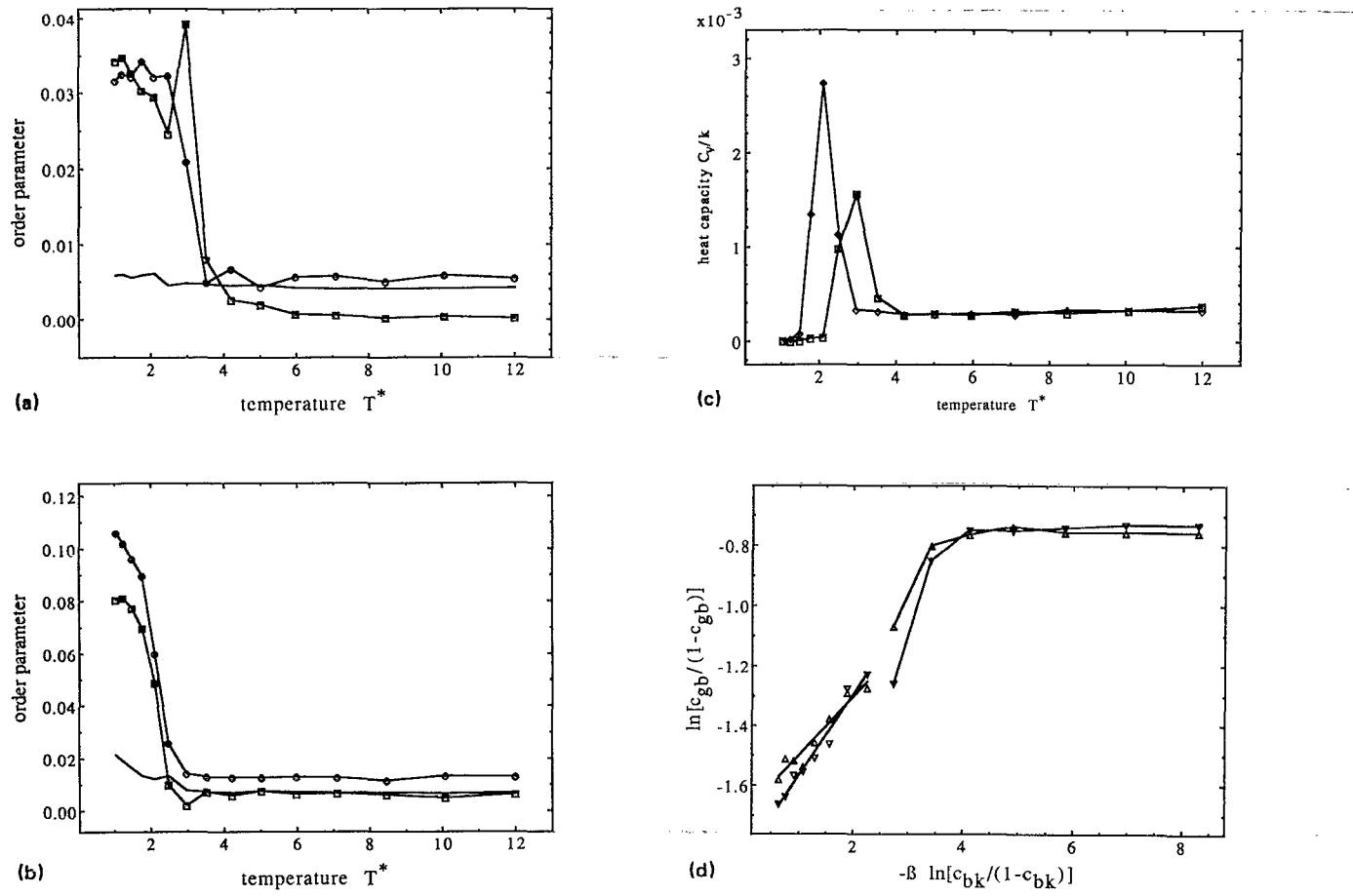

FIG. 6. Several order parameters used to analyze the Monte Carlo simulations. (a) is the Fourier order parameter Θ_λ [Eq. (22)] for the bulk canonical run which was depicted in Figs. 3(a)–3(c). Squares represent the $\lambda=2$ (antiferromagnetic) phase and circles represent the $\lambda=6$ phase. For background comparison, the curve without symbols shows the average Θ_λ when $\lambda=3$, 4, 5, 7, 8, and 9. (b) shows Θ_λ for the grain-boundary canonical run depicted in Figs. 5(a)–5(f), with symbols as in (a). (c) shows the heat capacity C_v [Eq. (23)] for the same bulk (squares) and grain-boundary (diamonds) canonical systems. The slope of (d) gives the binding energy according to the McLean segregation isotherm model [Eq. (24)] for the two grain boundaries run under the canonical ensemble. For one boundary (layers -9 to $+9$ inclusive, indicated by the upright triangles), the binding energy is 0.19 eV, while for the other the binding energy is 0.27 eV. The data have a linear fit at high temperature, but this simple model fails to account for the ordering phase transition which we observe at low temperature.

behavior near the boundary; a segregant peak with definite structure. Figure 5(b) shows how the segregant peak increases in both height and width with lower temperature, and the structure at the boundary becomes more pronounced. In spin language, this high-temperature behavior is primarily caused by variations in the magnetic field due to the asymmetrical nature of the boundary, favoring the acceptance of spin $+1$ (bismuth) near the boundary (see Fig. 4 in Ref. 3). At still lower temperature [Fig. 5(c)], the amount of segregant increases and the width of the peak increases well beyond the range of variations in the magnetic field. As detailed in our previous paper,[3] this effect can only be due to enhanced layer–layer coupling (see Fig. 3 in Ref. 3) at lower temperature.

With successively lower temperatures [Figs. 5(d)–5(f)], we clearly see that the ordered structure extends well beyond the tenth layer, which is the range of external field fluctuations, and displays the same ordered structure seen previously in the bulk simulations. We are observing for the first time here evidence of the keystone point of this paper; an ordering phase transition at a grain boundary can actually be a *bulk* phase transition that has nucleated at the boundary.

As with the bulk system, we calculate the Fourier coefficients of this concentration profile. Figure 6(b) shows the result of this order-parameter analysis, where we have excluded the 20 layers surrounding each grain boundary. Both the $\lambda=2$ (antiferromagnetic) and $\lambda=6$ phases appear at low temperature. From this graph, the transition temperature for these phases appears to be between 2.98 and 2.10. The next highest ordered phase (not shown in this figure) is $\lambda=7$, which was observed to be the most stable phase over a brief temperature range in mean-field theory.

Root-mean-square fluctuations of the energy give us an additional order parameter, the heat capacity [Eq. (23)], shown in Fig. 6(c). This graph indicates a phase transition temperature for this grain-boundary system around $T^*=2.10$, in contrast to the bulk system, where the transition temperature is ~ 3.

For the grain-boundary system, we introduce a third parameter to quantitatively indicate large-scale changes in the system. The McLean segregation isotherm,[21] predicts the degree of impurity segregation to a grain boundary and is commonly used by experimentalists seeking a theoretical fit to their data. It has the same general form as the Langmuir gas–surface adsorption isotherm,

$$\frac{c_{\text{g.b.}}}{1-c_{\text{g.b.}}}=\frac{c_{\text{bulk}}}{1-c_{\text{bulk}}}\exp(-\Delta G/RT), \tag{24}$$

where $c_{\text{g.b.}}$ and c_{bulk} are the equilibrium concentrations of the impurity in the grain boundary region and in the bulk region, and ΔG is the binding energy, that is, the Gibbs free energy difference between having an impurity atom in a grain boundary site and in a bulk site. This isotherm implicitly assumes a well-defined grain-boundary width, on which the value of ΔG will depend. We define the boundary region as the space where the magnetic field H_i takes on nonbulk values[3]; this results in a boundary which extends nine layers from the center interfacial layer.

Figure 6(d) graphs $\ln[c_{\text{g.b.}}/(1-c_{\text{g.b.}})]$ vs $-\beta\ln[c_{\text{bulk}}/(1-c_{\text{bulk}})]$. The slope of this plot gives the binding energy, ΔG. We do obtain a good linear fit from $T^*=12.00$ to 3.54 indicating that the segregation isotherm is a good model at high temperature. $T^*=3.54$, which corresponds to $\beta\ln[c_{\text{bulk}}/(1-c_{\text{bulk}})]=2.2$, was chosen because it is above the upper temperature limit for the bulk phase transition and because those points give the highest correlation fit for one of the grain boundaries. Thus, despite the ordered short-range structure near the boundary, which is caused by variations in the magnetic field, this simple one-parameter model does succeed to predict the high-temperature concentration behavior on a coarse scale.

From linear regression, we obtain the binding energy ΔG at these high temperatures as $\sim$0.18–0.28 eV. However, starting between $T^*=3.54$ and 2.98, the binding energy rises sharply. This behavior is consistent with our claim that the behavior at that point, although it happens near the grain boundary, is actually a bulk phase transition which overwhelms the spatially localized impurity segregation to the grain boundary. The binding energy rises dramatically because the temperature is low enough for layer–layer coupling to induce the bulk phase transition, with the boundary segregant serving as a nucleus. It then levels off when that region becomes saturated with the new bulk phase.

To summarize the results of the canonical grain-boundary simulations, we observe the interfacial segregation of bismuth. With decreasing temperature, the segregant peak broadens, the amount of segregant increases, and the segregant forms an ordered structure. Below a transition temperature approximately $T^*=2$–3, we also observe the appearance of the bulk phase. We clearly see that the ordered phase can be nucleated at the boundary. We propose this boundary-nucleated concentration-limited bulk phase transition as a mechanism for the boundary phase transition in the copper–bismuth system. This behavior should occur in any physical system where interfacial segregation is strong, where the potential favors bulk ordering, and when bulk solubility is low. The first condition assures us that a nucleus forms at the boundary, the second that an ordered structure will form, and the third that this ordered structure will selectively nucleate at the interface instead of across the entire system.

This is clearly a bulk, rather than a boundary, phase transition. In the language of spin models, the segregant peak at these temperatures extends well beyond the region where the magnetic field varies, so any structure of greater width must be due to spin–spin interactions. In addition, the ordered structure has wavelengths $\lambda=2$ and 6, identical to the stable bulk structures. By every measure, the ordered phase actually appears more definitively in the presence of the grain boundary compared with the bulk system alone. The clarity of the concentration profiles (Fig. 3 vs Fig. 5), the Fourier order parameter Θ_λ [Fig. 6(a) vs Fig. 6(b)], and the heat capacity C_v [Fig. 6(c)] all indicate that the phase transition is stronger in the presence of a grain boundary, supporting our notion that the interface serves as a nucleation site for the ordered phases.

Besides the concentration-profile Fourier coefficient, two other order parameters, the heat capacity and McLean segregation binding energy, indicate that a bulk ordered phase appears at approximately $T^*=2$–3. This transition temperature is lower than the canonical bulk phase transition temperature, but entirely consistent with the $\delta\mu$-gradient simulation, where the concentration also varies spatially and the transition temperature appears slightly lower than $T^*=3$. Finally, the nucleation of the bulk phase by boundary segregant was seen in our earlier mean-field analysis.

D. Vacancy-oriented kinetic canonical

To investigate the kinetics of the formation of this phase transition, we perform a number of vacancy-oriented kinetic Monte Carlo simulations. Unlike the previous simulations, instead of taking the system configuration from a high temperature as the initial state for the next lower temperature, we start each of these kinetic runs from a uniformly flat concentration profile. This method takes advantage of the algorithm's efficiency at low temperature and simulates the kinetic effect of rapid experimental quenching.

The system under this algorithm behaves at high temperature similar to the canonical simulation described in the preceding section. Down to $T^*=4.22$, the energy of this simulation closely matches the best Metropolis simulation, and the concentration profile shows the same segregant structure at the grain boundary and flat profile in the bulk. Below that temperature, however, the energy is higher than the canonical Metropolis simulation, and the concentration profile displays ordering across the entire simulation regardless of the location of the boundary. This behavior resembles the grand canonical simulation, in which the ordered phase forms wherever local concentration fluctuations nucleate the new phase. This situation also occurred in some of the canonical simulations with higher energy. In this kinetic simulation, the ordered phase also does not necessarily occur near the boundary, because

the vacancy first appears at a random location. Therefore, ordering first begins in the region near the vacancy instead of at the grain boundary, where the segregant could serve as a nucleus for ordering.

This kinetic algorithm indicates a precaution for the experimental study of grain boundary segregation and ordering. For a particular system, even if the high-temperature boundary segregation does not depend on careful annealing and quenching, the appearance of an ordered phase near the boundary at low temperature may be sensitive to the temperature history of the material. Thus, the system must be annealed to a temperature sufficiently low for boundary segregation, but sufficiently high so that the ordered phase has not yet appeared. The material must then be slowly cooled so that the ordered phase appears at the boundary instead of at randomly scattered locations through the crystal.

V. SUMMARY

These simulations illustrate the use of familiar and novel Monte Carlo techniques towards a difficult physical problem, confirm our earlier analytic theory,[3] and provide further insight into the basic nature of grain boundary segregation and ordering.

We have seen how the copper/bismuth potentials produce an ordered phase at low temperature. The appearance of this ordered phase in a finite system renders it difficult to control the concentration in the grand canonical ensemble. In particular, two simulations which modify the usual notion of the chemical potential difference $\delta\mu$, the concentration-dependent and spatially dependent $\delta\mu$-gradient simulations, indicate the problem. The presence of a grain boundary, on the other hand, produces inhomogeneous interactions. The broken symmetry of the lattice makes some regions richer in impurity concentration than others, depleting the bulk crystal, so a simulation in the canonical ensemble depends somewhat on size. Being careful to run a large enough simulation, we investigated the behavior of the grain boundary system with a Metropolis algorithm and with our vacancy-oriented kinetic algorithm.

These three dimensional simulations confirm every fundamental prediction from our one-dimensional mean-field theory. In the bulk, the $\lambda=2$ (antiferromagnetic) and $\lambda=6$ ordered phases appear at low temperature, and $\lambda=6$ is the more stable phase. Both theories also concur on the behavior of the grain-boundary segregant at high temperature, where the external field determines the shape of the impurity segregant peak. The peak increases in both width and height with lower temperature. Significantly, in both calculations the segregant peak serves as a nucleus for the bulk ordered phase.

Most importantly, these simulations further illuminate the relationship between boundary segregation, which has long been experimentally observed, and boundary phase transitions, which have only recently been indicated by experiment.[7] We observe two distinct temperature domains of increasing impurity concentration at the interface. In our system, the high-temperature behavior displays a considerably detailed structure, but its coarse behavior can still be described by a one-parameter segregation isotherm. At low temperature, the bulk ordered phase appears and can nucleate at the boundary. This phase transition occurs at the interface because of strong interlayer coupling, so the width of the segregant is limited only by the amount of bismuth that can migrate to the boundary. Since the solubility of bismuth in copper is low, in our system the segregant peak does not extend far into the bulk copper. The kinetic algorithm helps describe under what conditions this concentration-limited boundary-nucleated bulk phase can appear.

In summary, we suggest that this boundary nucleation may be a general mechanism for a class of boundary phase transitions and we expect these theoretical techniques may help experimentalists to identify physical systems with similar behavior.

[1] *Interfacial Segregation*, edited by W. C. Johnson and J. M. Blakely (Am. Soc. Metals, Metals Park, Ohio, 1977).

[2] J. B. Vander Sande, A. J. Garratt-Reed, Y. -M. Chiang, and T. Thorvaldsson, Ultramicrosc. **14**, 65-74 (1984); A. J. Garratt-Reed, Scanning Electron Microsc. **I**, 21 (1985).

[3] W. L. Alba and K. B. Whaley, J. Chem. Phys. **95**, 4427 (1991).

[4] For a collection of computer simulation techniques applied to solid–solid interfaces, see Surf. Sci. **144** (1984).

[5] See, for example, A. P. Sutton and V. Vitek, Acta Metall. **30**, 2011 (1982); J. T. Wetzel and E. S. Machlin, Surf. Sci. **144**, 124 (1984).

[6] S. -M. Kuo, A. Seki, Y. Oh, and D. N. Seidman, Phys. Rev. Lett. **65**, 199 (1990); S. M. Foiles and D. N. Seidman, MRS Bull. **15**, 51 (1990).

[7] M. Menyhard, B. Blum, and C. J. McMahon, Jr., Acta Metall. **37**, 549 (1989).

[8] J. P. Valleau, G. M. Torrie, and S. G. Whittington, in *Statistical Mechanics, Part A*, edited by B. Berne (Plenum, New York, 1977), Chap. 4 and 5.

[9] H. K. Chang, J. K. Lee, and D. F. Stein, in *Interatomic Potentials and Crystalline Defects*, edited by Jong K. Lee (Metallurgical Society of AIME, Warrendale, 1981), pp. 373–388; H. K. Chang, R. S. Weidman, and J. K. Lee, Surf. Sci. **144**, 224 (1984).

[10] K. Binder, in *Monte Carlo Methods in Statistical Physics*, edited by K. Binder (Springer, New York, 1986), pp. 1–45.

[11] R. J. Borg and G. J. Dienes, *An Introduction to Solid State Diffusion* (Academic, San Diego, 1988).

[12] L. A. Girifalco and V. G. Weizer, Phys. Rev. **114**, 687 (1959).

[13] A. Fraczkiewicz and M. Biscondi, J. Phys. (Paris) **46 C4**, 497 (1985).

[14] A. Roy, U. Erb, and H. Gleiter, Acta Metall. **30**, 1847 (1982).

[15] P. H. Pumphrey, in *Grain Boundary Structure and Properties*, edited by G. A. Chadwick and D. A . Smith (Academic, San Francisco, 1976), pp. 139–200.

[16] D. J. Chakabarti and D. E. Laughlin, Bull. Alloy Phase Diagrams **5**, 148, 203 (1984).

[17] T. Beck, J. Jellinek, and R. S. Berry, J. Chem. Phys. **87**, 545 (1987); H. L. Davis, J. Jellinek, and R. S. Berry, *ibid.* **86**, 6456 (1987); J. Jellinek, T. Beck, and R. S. Berry, *ibid.* **84**, 2783 (1986).

[18] K. Binder, Z. Phys. **267**, 313 (1974).

[19] J. W. Christian, *The Theory of Transformations in Metals and Alloys* (Pergamon, New York, 1965).

[20] J. M. Ziman, *Models of Disorder* (Cambridge University, Cambridge, 1979).

[21] For a review on segregation isotherms, see, for example, *Adsorption on Metal Surfaces*, edited by J. Bernard (Elsevier, New York, 1983) or S. Hofmann, Scanning Electron Microsc. **III**, 1071 (1985).